

## Minimum-pixel holograms

Stephen A. Benton and Ravikanth S. Pappu

MIT Media Laboratory

20 Ames Street

Cambridge, MA 02139 USA

### ABSTRACT

Canonical minimal-pixel hologram geometries are presented in the context of a generalized image relay system. We illustrate that the number of pixels ultimately depends only on the physical parameters of the displayed image (the Smith-Lagrange optical invariant). Various choices of synthetic optical geometries lead to pixel aspect ratios that are found to be good matches to available display technologies. We explore geometries in which the spatial light modulator is imaged at either the image-plane or the viewer-plane, or astigmatically imaged to both at the same time. This increases the variety of candidate aspect ratios considerably, and brings us closer to a workable match with foreseeable optical technologies that will make holographic video a practical reality.

### 1.INTRODUCTION

The problem of synthesizing free-standing spatial images has occupied the thoughts of researchers for over one and a half centuries. When optical holography was invented by Denis Gabor in 1949, it was thought that a satisfactory solution to the problem of creating autostereoscopic images was finally found. However, holography has several limitations that keep it from being a viable medium for the routine presentation of 3-D images. It seemed that the price that one had to pay for being able to see realistic three-dimensional images was to produce and view them under severely restricting conditions. Most of the restrictions arose from the use of coherent light to record and reconstruct the image.

In 1965, inspired by the work of Kozma and Kelly<sup>1</sup>, Brown and Lohmann<sup>2</sup> realized that holograms could be synthesized using computers by modeling the process by which optical holograms were recorded. A *computer-generated hologram* (CGH) may be defined as a numerical representation of an interference pattern. Once the physics of holography was known, it was a simple matter to produce CGHs. Some of the earliest CGHs were complex amplitude masks with applications in spatial filtering. The extension to computed display holograms is conceptually straightforward. However, simple calculations by Leith and his colleagues in 1965 showed that it would be impossible to compute display holograms because of the enormous number of samples involved. The possibility of producing CGHs that could be transmitted and reconstructed optically at a remote location in real-time was ruled out.

Recently, the Spatial Imaging Group at MIT reported the successful implementation of a system that could display a computer-generated holographic image in real-time. The engineering and computational

details of the display have been documented extensively elsewhere<sup>3, 4, 5</sup>. The MIT Holographic Video System (holovideo) accepts two inputs -- a CGH and light -- and produces a 3D image that is available in a predefined volume. In a sense, light obeys the instructions provided by the CGH to diffract light into the volume.

Consider holovideo in terms of the flow of information through the system. From Figure 1 below, it is clear that the same information is represented in various forms as it flows through the system. It should be noted that all the indicated quantities -- cycles, samples, bits, and pixels -- are not related in a simple way. The number of bits is directly proportional to the number of samples: these quantities are related via the number of bits per sample. However, minimizing the number of bits does not necessarily minimize the number of cycles. Shannon's channel coding theorem only shows that there exist good codes that can be decoded with exponentially small probabilities of error, but provides no method of constructing those codes. A code without some structure to it may take an infinite number of cycles to encode and decode. On the receiver's side, the number of pixels is equal to the number of samples that are decoded. Clearly, it is necessary to make a trade-off amongst these quantities.

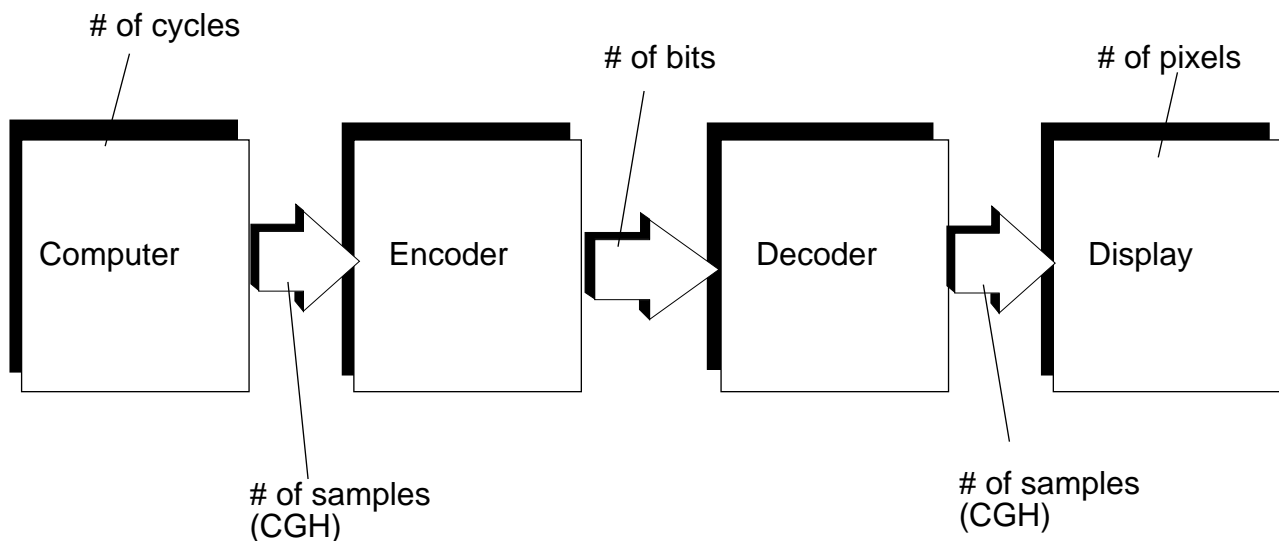


**Figure 1: Different representations of information in a holographic display**

In this paper, we are concerned exclusively with the physical format of information presentation to the beam of light. Typically, this requires some kind of spatial light modulator (SLM). In our system, we use an AOM. Other systems have used liquid crystal displays (LCDs). The physical format refers to the aspect ratio of the pixels of the modulator. We determine the pixel aspect ratios of computed holograms with the least number of pixels -- hereafter referred to as minimum-pixel holograms (MPHs). Our approach will be as follows. First, we present the generalized image relay system (GIRS) which is the context in which the MPHs will be discussed. Then we present canonical MPH geometries, determine aspect ratios for the pixels, and demonstrate that the total number of pixels depends only on the physical parameters of the displayed image. Cylindrical extensions of the GIRS are treated in section 4. The final section summarizes the paper and presents directions for future work.

## 2. THE GENERALIZED IMAGE RELAY SYSTEM

The GIRS is a simple two-lens relay system as shown in Figure 2. L1 and L2 are identical spherical lenses which are separated by twice their focal length ( $F$  mm). L1 is the *objective lens* and L2 is the *field lens*. L1 forms a real image of the three-dimensional scene in space. The primary function of L2 is to prevent vignetting of the image. It has no effect on the power of the system *per se*, but it bends rays which would otherwise leave the system back towards the axis. Another important function of L2 is that it corrects simple geometric distortions so that longitudinal and lateral magnifications of the image are independent of  $z$ -location. The connection between this system and holography is the subject of the rest of this section.

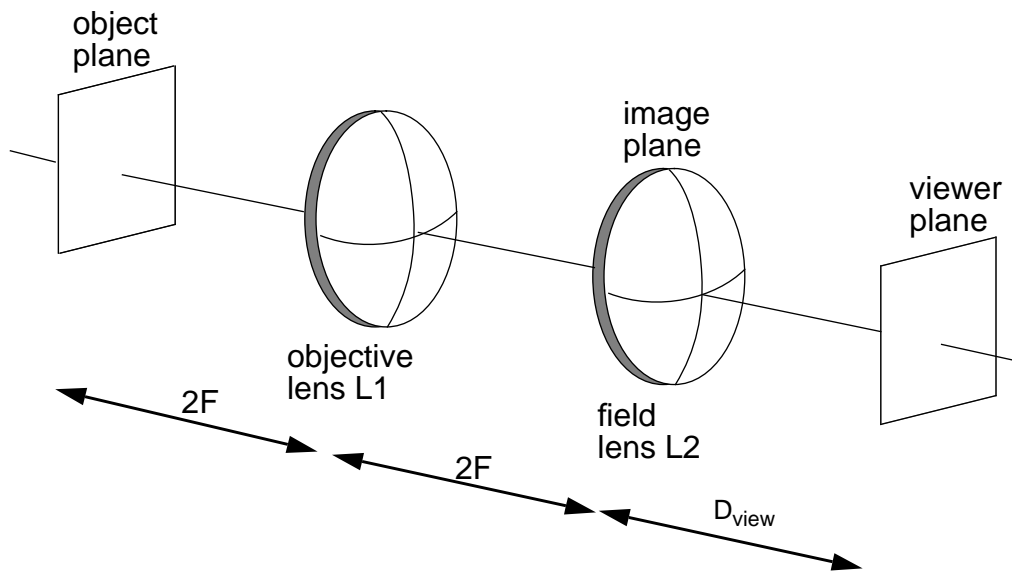


**Figure 2: The Generalized Image Relay System**

To model a hand-held holographic image viewing situation, the images are taken to be 100 mm on a side and the viewing distance is 500 mm. This implies that the lenses have a focal length of 250 mm, and a diameter of 141 mm. Their f-number is 1.8. The magnification is taken to be unity without loss of generality. Consider inserting a holographic plate at some plane in the system and recording a hologram in that plane. All components downstream of the plate may be removed in the recording process. The image may then be reconstructed from that hologram by “playing it back” through the rest of the system. This is shown in Figures 3a and 3b. If the hologram were recorded just before or after the field lens L2, it would bisect the image of the three-dimensional scene. This is the equivalent of an *image-plane hologram* in which the viewer looks *at* the hologram. The other extreme, a *viewer-plane hologram*, can be recorded by putting the hologram plane just before or after the objective lens L1. Lens L2 would image the hologram to the viewer’s plane, who would look *through* it at the image. The location of the hologram plane between L1 and L2 is a free variable -- a dial -- by which the hologram may be recorded as an image-plane hologram, a viewer-plane hologram, or anything in between.

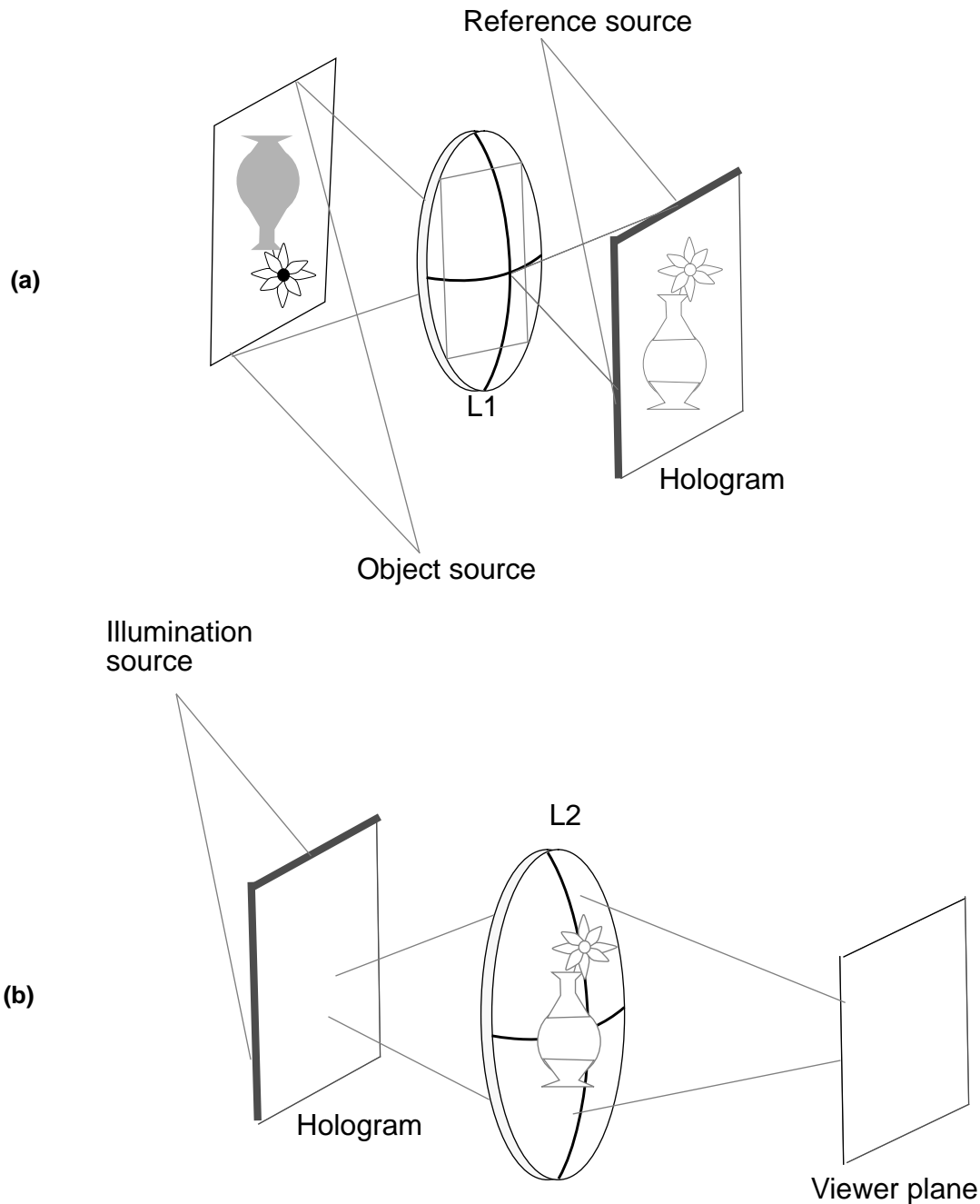


**Figure 3: (a) Recording and (b) reconstruction of the hologram in a GIRS**

The GIRS may also be used to model and analyze *horizontal parallax only* (HPO) imaging situations. This is shown in Figure 4. Reduction of vertical parallax is achieved by using a horizontal slit in the plane of L1, much like in a rainbow hologram. The slit permits only a side-to-side range of perspectives to enter the system. The view-zone is now an aerial image of the slit. A vertical diffusing element must be provided after L2 in order to make the view-zone usable. The introduction of the slit brings with it *astigmatism* in deep images, a feature of any HPO imaging scheme. It occurs because vertical information is always centered at the surface of the diffuser while horizontal information is centered at

the apparent viewing distance. Astigmatism limits the usable depth of the image.

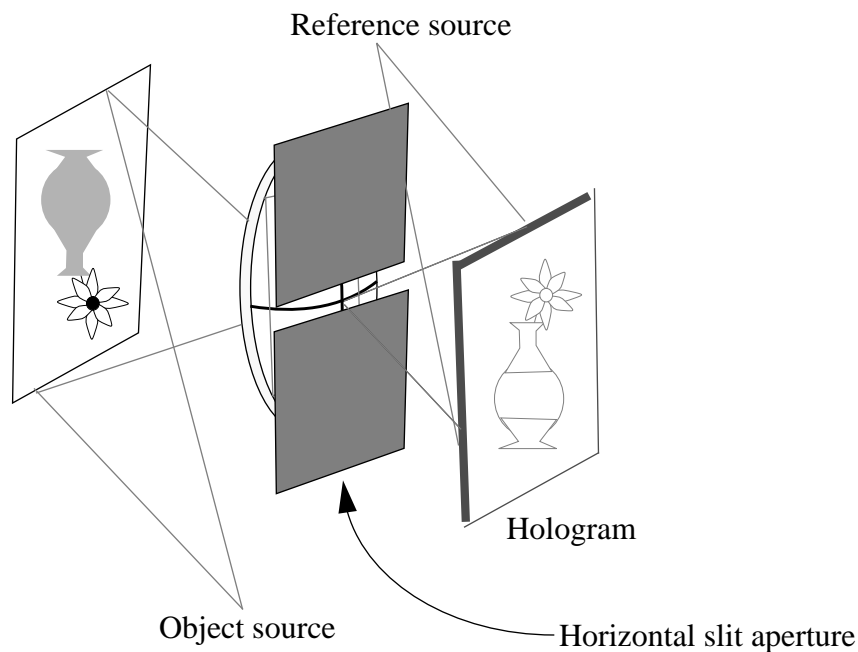


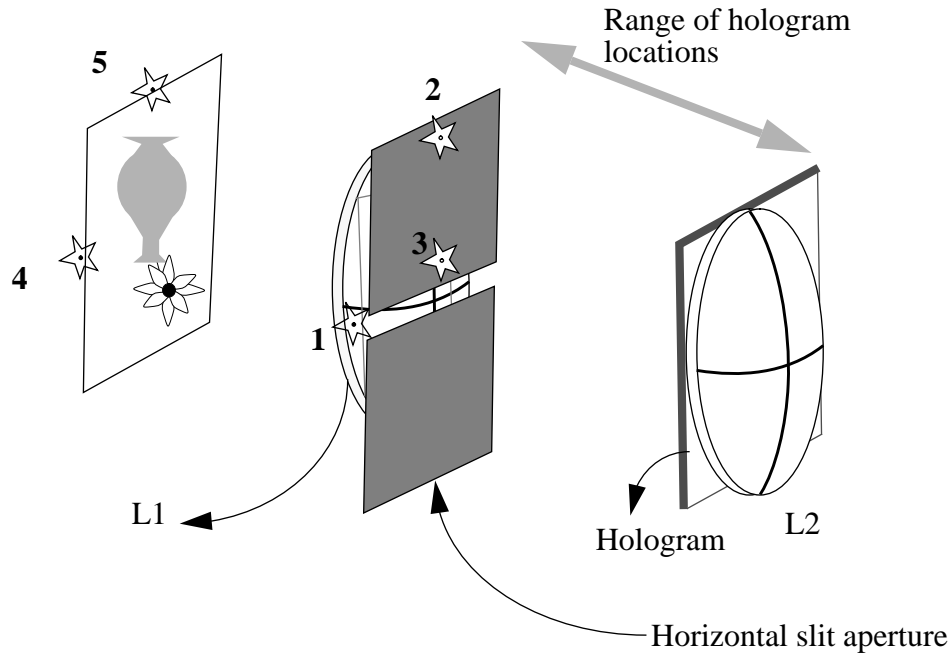
**Figure 4: Recording an HPO hologram in the GIRS**

The location of the hologram plane is one degree of freedom. Another degree of freedom is the location of the reference source. The recording of an image-plane HPO hologram is shown in Figure 5. The hologram plane is just after L2 and the reference source is placed at the end of the slit. In optical holography, the source would be placed at least the width of the slit from its end, but this is not a restriction in computer-generated holography, because the “halo” term can explicitly be excluded in the computation. The position of the reference source is chosen so as to keep the maximum spatial frequency of the hologram transmittance pattern approximately constant over the hologram area. If the reference source were in a different location or produced plane waves, the maximum spatial frequency would vary across the hologram area. Consideration of the consequences of varying spatial frequency is deferred for further study. In the following section, we take a closer look at canonical minimum-pixel hologram geometries and determine pixel aspect ratios in these cases.

### 3. CANONICAL MINIMUM-PIXEL HOLOGRAM GEOMETRIES

Canonical MPH geometries refer to either image-plane or viewer-plane hologram configurations. As was noted before, there are two degrees of freedom involved: the location of the hologram plane and geometry of the reference beam. In this section, we explore all possible combinations of hologram location and reference beam geometry. In the interest of brevity, only the image-plane case will be considered completely; the viewer-plane case will be outlined and only results will be stated.

*Full parallax image-plane holograms:* There are two possible reference source locations, as shown in Figure 5. They are designated 1 and 2 as shown.



| Hologram location | Reference source locations | Hologram type              | Slit |
|-------------------|----------------------------|----------------------------|------|
| L2                | 1,2                        | Full parallax image-plane  | ✗    |
| L2                | 1,3                        | HPO image-plane            | ✓    |
| L1                | 4,5                        | Full parallax viewer-plane | ✗    |
| L1                | 4,5                        | HPO viewer-plane           | ✓    |

**Figure 5: Locations of reference beam sources and hologram plane**

Consider the case when the source is in position 1. The pixel dimensions depend only on the sampling rates in the hologram plane, which in turn depend only on the maximum spatial frequencies in the  $x$  and  $y$  directions. These spatial frequencies are designated  $f_{x,max}$  and  $f_{y,max}$ . Consider a point source at 1 and another point source traversing the semi-perimeter of a square aperture of side  $D$  mm, as shown in Figure 6a. Figure 6b shows the variation of  $f_y$  vs.  $f_x$  as the point goes around the path. Clearly,  $f_y = f_{y,max}$  when the second point is directly above the first point. We use this fact to determine the maximum spatial frequencies as follows. Let  $\theta_{H,max}$  and  $\theta_{V,max}$  be the maximum angles subtended at

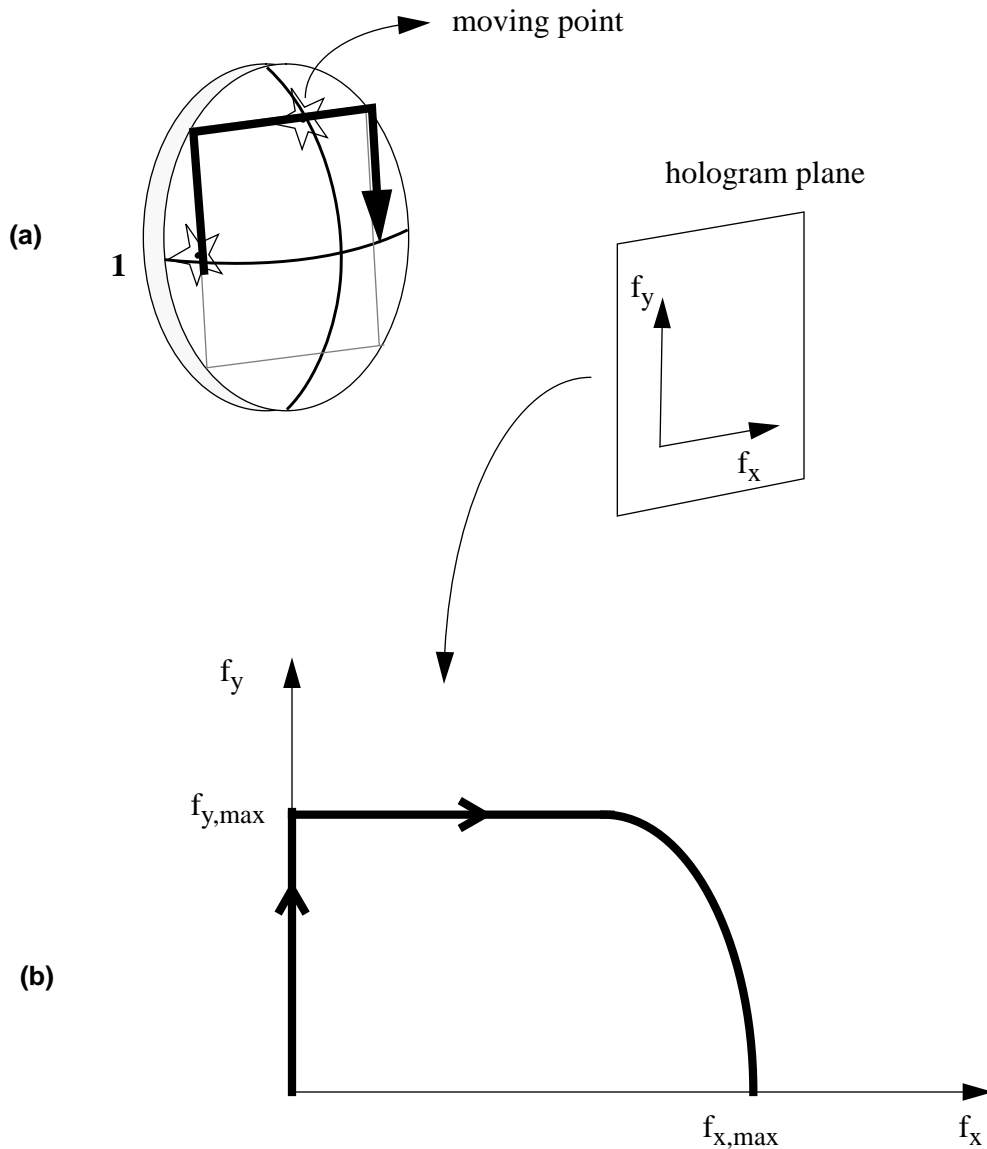


**Figure 6: (a) Two points on the perimeter of the aperture - one stationary and the other moving and (b) the spatial frequencies in the x and y directions**

the hologram plane in the  $x$  and  $y$  directions respectively. Then the following equations are true.

$$\begin{aligned}\theta_{H,max} &= 2 \tan^{-1} \left( \frac{D}{4F} \right) \\ \theta_{V,max} &= \tan^{-1} \left( \frac{D}{4F} \right)\end{aligned}\tag{1}$$

where  $F$  is the focal length of either L1 or L2. Therefore, the maximum spatial frequencies in both directions are given by:

$$\begin{aligned}
f_{x, max} &= \frac{\sin(\theta_{H, max})}{\lambda} \\
f_{y, max} &= \frac{\sin(\theta_{V, max})}{\lambda}
\end{aligned}
\text{ line pairs per mm} \tag{2}$$

where  $\lambda$  is the wavelength of light used to record the hologram. Recognizing that the hologram transmittance pattern must be sampled at twice the maximum spatial frequency in either direction, following the prescription of the Shannon-Nyquist sampling theorem, we determine the number of samples in each millimeter of the hologram. The dimensions of each pixel follow trivially from the number of samples per unit length. Let us label the pixel dimensions  $p_x$  and  $p_y$ . Then:

$$\begin{aligned}
p_x &= \frac{\lambda}{2 \sin(\theta_{H, max})} \\
p_y &= \frac{\lambda}{2 \sin(\theta_{V, max})}
\end{aligned}
\text{ mm} \tag{3}$$

If the dimensions of the hologram are  $P \times Q$  mm, then the total number of pixels required is

$$N_{full-parallax, A} = \left(\frac{4}{\lambda^2}\right) (PQ) \sin(\theta_{H, max}) \sin(\theta_{V, max}) \tag{4}$$

This is the *space-bandwidth product* (SBWP) or the *Smith-Lagrange optical invariant* of the hologram. Clearly, the SBWP depends on the hologram area and the angles subtended at the hologram, as expected. Any full parallax hologram recorded in the GIRS will have exactly the same number of pixels. Evaluating (3) and (4) for a test case using  $F = 250\text{mm}$ ,  $D = 100\text{mm}$ , and  $\lambda = 633\text{nm}$ , we obtain  $p_x = 1.6\mu\text{m}$ ,  $p_y = 3.2\mu\text{m}$ , and  $N_{full-parallax, A} = 1.96 \times 10^9$  samples. This is a prohibitive number of samples and was one of the primary factors in discouraging holovideo research in the early days of holography. The aspect ratio of these pixels is 1:2.

*HPO image-plane holograms:* In the previous case, we computed the pixel dimensions for each axis independently. This is a useful approach, because it simplifies the computation for the HPO case. The horizontal dimension of the pixel remains exactly the same. The only change is in the vertical dimension, because we don't require diffraction in the vertical direction. If we require  $L$  lines in the hologram, then the vertical dimension becomes  $p_y = Q/L$  mm. For our example,  $p_y$  becomes  $390\mu\text{m}$ , giving an aspect ratio of 1:244. In this case, we require pixels which are much taller than they are wide, which matches our intuition about HPO holograms.

If the reference source is now moved to position 2 (Figure 5), the pixel aspect ratios are simply transposed for the full parallax case. For the HPO case, they become  $3.2\mu\text{m} \times 390\mu\text{m}$ , giving an aspect ratio of 1:122. A similar analysis may be performed for the viewer-plane case. Pixel aspect ratios for all canonical MPH geometries are presented in Tables 1 and 2 below. At first glance, it appears that the SBWP is not the same for the image-plane and viewer plane cases in Table 2, because the pixels are much smaller in the viewer-plane case. This is obviously not true, and the reason lies in the fact that the



viewer-plane HPO hologram has a *smaller area* than a corresponding image-plane HPO hologram. The fact that the SBWP is invariant in both cases can be used to determine the slit height. In this case, the slit height is 0.82 mm, which exactly matches the value derived from Fourier considerations<sup>6</sup>.

**Table 1: Full parallax holograms**

| Hologram Type | Reference source location | Pixel dimension ( $\mu\text{m}$ ) | Pixel aspect ratio |
|---------------|---------------------------|-----------------------------------|--------------------|
| Image-plane   | 1                         | $1.6 \times 3.2$                  | 1:2                |
|               | 2                         | $3.2 \times 1.6$                  | 2:1                |
| Viewer-plane  | 4                         | $1.6 \times 3.2$                  | 1:2                |
|               | 5                         | $3.2 \times 1.6$                  | 2:1                |

**Table 2: HPO holograms**

| Hologram Type | Reference source location | Pixel dimension ( $\mu\text{m}$ ) | Pixel aspect ratio |
|---------------|---------------------------|-----------------------------------|--------------------|
| Image-plane   | 1                         | $1.6 \times 390$                  | 1:244              |
|               | 3                         | $3.2 \times 390$                  | 1:122              |
| Viewer-plane  | 4                         | $1.6 \times 3.2$                  | 1:2                |
|               | 5                         | $3.2 \times 1.6$                  | 2:1                |

#### 4. CYLINDRICAL EXTENSIONS OF THE GIRS

It is clear that the variety of pixel aspect ratios is considerable when HPO imaging is taken into account. In this section we examine cylindrical optical extensions of the GIRS and determine the pixel aspect ratios. Our motivation for studying the cylindrical case is the following. First, the variety in pixel aspect ratios is broadened. Second, there is an additional degree of freedom when cylindrical lenses are used, which provides the ability to control the amount of astigmatism. Finally, the dynamic range requirement on the samples may be relieved in this case but this problem is deferred for future study. We will consider the most practical case in which the image of the modulator is in the image-plane.

Consider Figures 7a and 7b. Figure 7a represents the vertical subsystem while Figure 7b represents the horizontal subsystem. Our goal is to set up a geometry such that the image is anastigmatic and the image

of the hologram is astigmatic. This means that horizontal and vertical image information are focused at lens LV4. The hologram plane is located at lens LV2. Horizontal hologram information is focused at LV4 while vertical hologram information is focused at the viewer-plane - the hologram is imaged to two different planes. From the discussion in section 3, it is clear that this arrangement produces an image-plane hologram as far as horizontal hologram information is concerned and a viewer-plane hologram for the vertical hologram information. This is clear from Figures 7a and 7b where the viewer looks *at* the horizontal hologram and *through* a vertical hologram at an anastigmatic image. There are four possible reference source locations - A, B, C, D - as shown in Figures 7a and 7b. We use an analysis similar to the one in section 3 to determine pixel aspect ratios for both the full parallax and HPO cases.

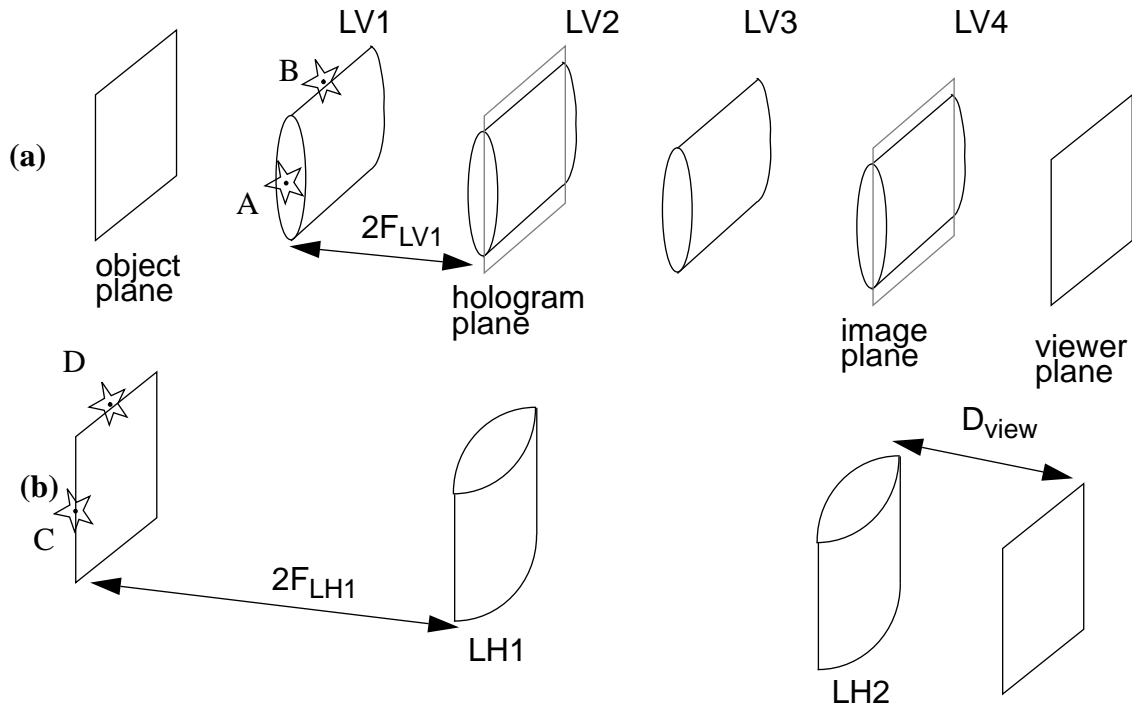


**Figure 7: (a) The vertical subsystem of the cylindrical GIRS and (b) the horizontal subsystem. Note that the image is anastigmatic while the two holograms are spatially separate. The locations of the reference beams are A, B, C, and D.**

The results are summarized in Tables 3 and 4. We use the same argument that precedes Figure 6 to determine the aspect ratios. It must be noted that lens LH2 has a different focal length than that of lens LH1. If we assume that the viewing distance is  $D_{view}$ , then we have the following relationship for the required focal length.

$$f_{LH2} = \frac{2D_{view}F_{LH1}}{2F_{LH1} + D_{view}} \quad (5)$$

Continuing our previous example, with  $D_{view} = 500mm$ , we have  $F_{LH2} = 250mm$ .

**Table 3: Full Parallax Holograms**

| Reference source location | Pixel dimension ( $\mu m$ ) | Pixel aspect ratio |
|---------------------------|-----------------------------|--------------------|
| A                         | $1.6 \times 1.8$            | 1:1.125            |
| B                         | $0.852 \times 1.6$          | 1:1.880            |
| C                         | $1.6 \times 0.823$          | 1:0.514            |
| D                         | $1.6 \times 0.852$          | 1:0.532            |

For the HPO case, we interpose a horizontal slit aperture at lens LV2 that allows only a limited vertical perspective. A vertical diffusing element is located in the plane of lens LV4. In this case, the vertical pixel dimensions are determined by the number of lines required in the hologram. For our example, the number of lines is 256, as before. We also use the same slit width as before: 0.82 mm. This leads to the entries in Table 4. For purposes of comparison, we note that some of the newest LCDs from Epson have aspect ratios between 1:1 and 1:3.

**Table 4: HPO Holograms**

| Reference source location | Pixel dimension ( $\mu m$ ) | Pixel aspect ratio |
|---------------------------|-----------------------------|--------------------|
| A                         | $1.6 \times 3.2$            | 1:2                |
| B                         | $0.852 \times 3.2$          | 1:3.75             |
| C                         | $1.6 \times 3.2$            | 1:2                |
| D                         | $1.6 \times 3.2$            | 1:2                |

## 5. SUMMARY AND CONCLUSIONS

Aspect ratios for MPHs were computed in the above two sections. It is clear that the variety of aspect ratios is increased when a cylindrical extension to the GIRS is used. Using a cylindrical GIRS enables us to have an extra degree of freedom -- the ratio of the focal lengths of the two types of cylindrical lenses. An approach where the image is anastigmatic while the two hologram planes are separated in space was presented. A related approach was followed by Fritzler and Marom<sup>7</sup> in their quest to reduce the information content of a holographic image. It must be mentioned that Vanderlugt<sup>8</sup> also performed a careful analysis of the spatial frequencies at different planes in the system and concluded that different pixels in the same plane should have different dimensions. Our paper deals with samples which have the same dimensions all over the plane, keeping a practical system in mind. It must be noted that careful analyses of dynamic range requirements for computed holograms -- near-field holograms in particular -- have not been done. This problem is the subject of study at this time.

## 6. ACKNOWLEDGMENTS

The authors acknowledge valuable discussions with Mark Lucente and Michael Klug and thank members of the Spatial Imaging Group for suggestions. Components of this research have been sponsored by the Television of Tomorrow research consortium of the Media Laboratory, MIT; Honda Research and Development Co., Ltd.; NEC Corporation; International Business Machines Corp.; and the Advanced Research Projects Agency (ARPA) through the Naval Ordnance Station, Indian Head, Maryland (under contract No. N00174-91-C0117)

## 7. REFERENCES

- [1] Kozma, A. and Kelly, D. L., *Spatial Filtering for Detection of Signals Submerged in Noise*, Applied Optics 4, 387 (1965).
- [2] Brown, B. R., and Lohmann, A. W., *Complex Spatial Filtering with Binary Masks*, Applied Optics 5, 967 (1966).
- [3] Lucente, Mark., *Diffraction-Specific Fringe Computation for Electro-Holography*, Ph.D Thesis, Electrical Engineering and Computer Science Department, Massachusetts Institute of Technology, 1994.
- [4] St. Hilaire, Pierre., *Scalable Optical Architectures for Electronic Holography*, Ph.D Thesis, MIT Program in Media Arts and Sciences, Massachusetts Institute of Technology, 1994.
- [5] Sutter, John., *Viewer-Plane Experiments with Computed Holography with the MIT Holographic Video System*, SM Thesis, MIT Program in Media Arts and Sciences, Massachusetts Institute of Technology, September 1994.
- [6] Benton, S. A., *Experiments in Holographic Video Imaging*. SPIE Institute Series Vol. IS 8 1990.
- [7] Fritzler, D., and Marom, E., *Reduction of Bandwidth Required for High Resolution Hologram Transmission*, Applied Optics, Vol. 8, No. 6, June, 1969.
- [8] Vanderlugt, A., *Optimum Sampling of Fresnel Transforms*. Applied Optics, Vol. 29, No. 3, 10 August, 1990.